NASA TECHNICAL MEMORANDUM NASA TM-76606

EXPERIMENTAL STUDY OF THE INTERACTION BETWEEN THE WING OF A SUBSONIC AIRCRAFT AND A NACELLE OF A HIGH BY-PASS RATIO ENGINE

P. Levart

Translation of "Etude Experimentale de l'Interaction entre une Voilure d'Avion Subsonique Rapide et une Nacelle de Moteur a Haut Taux de Dilution", IN: AGARD Subsonic/Transonic Configuration Aerodynamics, AGARD Conference Proceedings no. 285, Advisory Group for Aerospace Research and Development, Neuilly-sur-Seine, France (presented at the Fluid Dynamics Panel Symposium), Munich, May 5-7, 1980, pp. 20-1 to 20-11.

NATIONAL AERONAUTICS AND SPACE ADMINISTRATION
WASHINGTON, D. C. 20546 JULY 1981

80A 40803

Standard Title Page

1. Report No. NASA TM-76606	2. Government Accession No.	3. Recipient's Catalog No.
4. Title and Subtitle: EXPERIMENTAL STUDY OF THE INTERACTION BETWEEN THE WING OF A SUBSONIC AIRCRAFT AND A NACELLE OF A HIGH BY-PASS RATIO ENGINE		5. Report Date JULY 1981 6. Performing Organization Code
7. Author(s) P. Levart		8. Performing Organization Report No. 10. Work Unit No.
9. Performing Organization Name and Address SCITRAN Box 5456 Santa Barbara, CA 93108		11. Contract or Grant No. NASw-3198 13. Type of Report and Period Covered Translation
12. Sponsoring Agency Name and Address National Aeronautics and Space Administration Washington, D.C. 20546		14. Sponsoring Agency Code

15. Supplementary Notes
Translation of "Etude Experimentale de l'Interaction entre une Voilure d'Avion Subsonique Rapide et une Nacelle de Moteur a Haut Taux de Dilution", IN: AGARD Subsonic/Transonic Configuration Aerodynamics, AGARD Conference Proceedings no. 285, Advisory Group for Aerospace Research and Development, Neuilly-sur-Seine, France (presented at the Fluid Dynamics Panel Symposium), Munich May 5-7 1980. pp 20-1 to 20-11.

16. Abstract
The oncoming of a new generation of subsonic transport aircraft (with supercritical wing and high by-pass ratio turbofans) has led to an experimental study of wing nacelle jet pylon interference in transonic flow. To this end, a test set-up was developed at the ONERA S3Ch wind tunnel. The nacelle models represent a turbofan by means of two compressed air jets. The scale is 1/18.5. The nacelles are fixed on a thrust balance measuring afterbody thrust and discharge coefficients. The wing is located between the sidewalls of the test section. Pressures are measured through 456 holes located on 8 airfoils. Drag coefficient of the wing is obtained by wake survey. The following parameters can vary (1) wing/nacelle position; (2) upstream Mach number (from 0.3 to 0.8); (3) jet pressure ratio; (4) with/without pylon and (5) type of nacelle. Wing nacelle interference can be studied by means of total thrust drag analysis as a function of the various parameters. The test set-up is described and examples of results are presented illustrating the possibilities of this set-up.

17. Key Words (Selected by Author(s))		18. Distribution Statement: Unclassified - Unlimited	
19. Security Classif. (of this report) Unclassified	20. Security Classif. (of this page) Unclassified	21. No. of Pages 27	22. Price

EXPERIMENTAL STUDY OF THE INTERACTION BETWEEN THE WING OF A SUBSONIC AIRCRAFT AND A NACELLE OF A HIGH BY-PASS RATIO ENGINE*

P. Levart**

***/20-1

SUMMARY

The oncoming of a new generation of subsonic transport aircraft (with supercritical wing and high by-pass ratio turbofans) has led to an experimental study of wing-nacelle-jet-pylon interference in transonic flow. To this end, a test set-up has been developed at the ONERA S3Ch wind-tunnel.

The nacelle models represent a turbofan by means of two compressed air jets. The scale is 1/18,5. The nacelles are fixed on a thrust balance measuring afterbody thrust and discharge coefficients.

The wing is located between the sidewalls of the test section. Pressures are measured through 456 holes located on 8 airfoils. Drag coefficient of the wing is obtained by wake survey.

The following parameters can vary:
- wing/nacelle position;
- upstream Mach number (from 0.3 to 0.8);
- jet pressure ratio;
- with/without pylon;
- type of nacelle.

---

* AGARD Conference Proceedings no. 285. Subsonic/Transonic Configuration Aerodynamics. Paper presented at the Fluid Dynamics Panel Symposium at the Munich Institute of Technology (illegible).

** Office National d'Etudes et de Recherches Aerospatiales, 29, avenue de la Division Leclerc, 92320 CHATILLON - FRANCE

*** Numbers in margin indicate pagination of foreign text.

Wing nacelle interference can thus be studied by means of total thrust-drag analysis, as a function of the various parameters.

The test set-up is described, and examples of results are presented illustrating the possibilities of this set-up.

/20-2

1. INTRODUCTION

The problem of nacelle-wing interaction on civilian aircraft has been discussed over the last few years by many authors [1-13]. Only a few studies consider the case of supercritical wings, which could be more sensitive to interactions than classical wings, or the case of nacelles of motors with a high dilution rate, which have a large dimension blower, which means that the nacelle has to be very close to the wing.

A rather general study of the nacelle-jet wing interaction was, therefore, undertaken in a wind tunnel in order to develop basic information required for selecting the relative nacelle-wing position for this type of configuration.

2. METHOD AND TEST EQUIPMENT

The tests were performed in the S3 wind tunnel at Chalais-Meudon at the ONERA.

2.1 S3 wind tunnel of Chalais-Meudon

This is a subsonic/transonic wind tunnel which is continuous and reversible. The cross section is quasi-octagonal. The dimensions of the test section are the following: Height 0.8m, width 0.9m. Diameter of the inscribed circle = 1m (area = 0.66 m^2). The total length of the test section is 1.75m and the useful length corresponds to the dimensions of the portholes: 0.60m. The generating pressure is close to the atmospheric pressure. The generating temperature increases as a function of Mach number, from ambient

temperature up to 340 K approximately for M = 0.9.

The lateral walls are solid and parallel (these are the portholes).

For this study, the upper and lower walls are solid, so that the incidence (angle) induced by wall effects is small. Initial tests in an empty wind tunnel carried out for Mach numbers between 0.3 and 0.9 gave satisfactory results. During the detailed tests discussed here, the Mach number upstream never exceeded 0.80.

2.2 Rear body weighing balance

Most of the experimental studies of the nacelle-wing interaction carried out up to the present time were designed to evaluate the influence of the presence of the propulsion nacelle (simulated more or less) on the wing characteristics. One of the original features of the present study is that in addition, we measured the influence of the presence of the wing on the engine performance as a function of various parameters. For this purpose, the propulsion nacelle is placed on a weighing balance for the rear body which is particularly designed for steadying the rear body of engines at a high dilution rate.

The diagram is shown in Figure 1.

The principle is the principle of an upstream sting where the model to be studied is fixed downstream of an axial cane which is used to provide compressed air flux and for the pressure measurement tubes. The balance used is a single component balance (axial thrust) and contains a dynamometric bar equipped with strain gauges.

The nacelle model consists of a part which is not weighed (inlet air fairing up to a coupling piece) and a weighed part (rear body proper).

In the first version, the connection between the weighed part and the non-weighed part was provided by an annular dynamometer located in the upstream part of the nacelle. The first tests showed difficulties with this arrangement. The space allowed for the dynamometer was tight , and it was anchored to not enough material. In the test, mechanical and thermal stresses developed so that a precise measurement of the thrust became impossible.

After this, the dynamometer was moved to the upstream point of the cane and the suspension between the weighed part and the non-weighed part is divided by an annular roller.

The control of the boundary layer along the sting upstream of the nacelle is provided by two devices which operate successively and simultaneously: One tangential blowing device and one aspiration device to the right of the inlet fairing. These two devices allow one to reduce the thickness of the boundary layer over the rear body and to reproduce a realistic external flow.

2.3 Test models

2.3.1 Wing

The wing model is shown in Figure 2. This is a wing with a chord of 220 mm with a relative thickness of 12.5%. It is installed with a sweepback angle of 28° between the lateral walls of the wind tunnel. The profile is an SNIAS profile of the supercritical type. The wing is twisted linearly by 3° along the width of the test section. The model is equipped with 456 wall pressure taps distributed into 8 sections. For each section there are 30 taps on the top side and 27 taps on the bottom side.

/20-3

In addition, the drag of the wing can be determined from soundings of the wake. Stagnation pressure explorations were performed for six chord positions corresponding to the wing sections carrying the wall pressure taps.

Wake pressure and wall pressures are not acquired simultaneously. The rake remains installed in the wind tunnel (in the retracted state) during the entire duration of the test. It is, therefore, important to verify that the presence of a rake does not noticeably influence the pressures measured over the wing. Figure 3 shows a pressure distribution measured over the wing with and without a rake downstream.

The tests were performed by artificially triggering the transition of the boundary layer using carborundum grains glued near the leading edge of the wing, on the top side and on the bottom side. The transition band with a width of 3 mm is placed 13.6 mm from the leading edge.

The wing is fixed between the walls of the test section, but its incidence angle can be changed, as can its altitude and its longitudinal position.

2.3.2 Nacelles

The nacelle models were provided by SNECMA. They faithfully represent at a scale of 1/18.5, solutions considered for the rear body of an engine with a high dilution rate, the CFM 56.

The thrust is obtained from two compressed air jets which simulate the engine flux.

Three models of nacelles were tested. They are shown in Figure 4. Two nacelles have confluent flux. One is short (FCC) and the other is long (FCL). The third one is of the short kind with separate flux (FSC).

They are equipped with pressure taps over the upper meridian of the external fairing.

2.3.3 Pylons

The mast which connects the propulsion nacelle to the wing plays a very important role in the wing-nacelle interaction. In any experimental study it is, therefore, important to represent these masts in a realistic manner. The mast was represented for four configurations, two with the FCL nacelle, one with the FCC nacelle and one with the FSC nacelle.

The masts are originally connected to the wing. Since the nacelles are weighed, there can be no mechanical contact between the mast and the nacelle. This explains the space between the nacelle and the mast.

The complete installation for the nacelle-wing interaction study is shown in Figure 5.

2.4 Tested configurations

Tests were performed in three stages.

a) after determining the incidence angle to use we studied the characteristics of the wing alone in the wind tunnel for different Mach numbers.
b) study of the thrust and the external pressure distributions of the three nacelles, tested alone in the wind tunnel.
c) study of the nacelle-jet-wing-pylon interaction with a simultaneous test of the wing and the axis.

This latter part then consists of several parts:

- influence of the delay rate of the jet engine on the wing characteristics
- influence of upstream Mach number
- influence of the relative wing/nacelle position
- influence of the nacelle type
- influence of the presence of the pylon

The influence of the delay rate was studied for values between the natural flow rate (that is, which simulates the jet emerging from a hollow nacelle) up to cruise conditions.

The upstream Mach number varies between 0.3 and 0.8.

For each of the nacelles FSC and FCC, several relative positions were studied. They define a T with three positions along the horizontal and two or three along the vertical. These positions are defined in Figures 6 and 7. The nacelle FCL was tested for two relative positions, both with the mast. These positions are defined in Figure 8.

The study of the influence of the presence of the pylon was performed for one relative position with the nacelle FSC (number 21') and another one with the nacelle FCC (number 18').

3. EXAMPLE OF RESULTS

The present test configuration allows one to acquire a great deal of information about the nacelle-wing interaction: Pressure distribution over the wing and over the nacelles, measurement of the thrust and the flow rate coefficient of the engines. For each configuration it is then possible to determine a thrust-drag global balance. The results which follow give an idea of the possibilities with the installation.

/20-4

For the analysis, the results were corrected for wall effects using the theory discussed in [14] by using a constant incidence angle and Mach number within the test section.

For each section, the aerodynamic coefficients were obtained by integration of the pressure measurements. The global C_x * and C_z

* The wake soundings were performed during a second test series. When this present document was edited, the results of the C_x of the wake were not yet available and the evaluation of the C_x was performed from the integration of pressures over the wing.

values of the wing were obtained by integrating the C_x and the C_z local values as a function of chord. It is found that the global coefficients only affect the part of the wing between the two extreme positions of the pressure tap .

3.1 Influence of the jet

A simple way of representing complete configurations of wings equipped with nacelles now in use consists of using a hollow nacelle through which a natural air flow rate circulates. It is then interesting to verify whether this representation is not too simplistic, by testing the wing plus nacelle combination for various air flow rates, from the natural flow rate up to the flow rate which represents the cruise thrust. This is done by comparing the local and global aerodynamic coefficients. Figure 9 shows that a substantial variation in the delay flow rate of the jet results in a very small variation of C_x and a moderate one in C_z. These results confirm the ones obtained by El-Ramly and Rainbird [15] for a similar configuration.

These tests show that it is interesting to use permeable nacelles when we are only interested in the wing characteristics.

On the other hand, the thrusts obtained with a natural flow rate and for the cruise flow rate are very different as are the pressure distributions over the nacelle fairing, especially over the cover of the first motor which is directly subjected to the influence of the jet on the lift and the drag of various sections in the chord direction for different Mach numbers.

In addition, Figures 11 and 12 show the influence of the delay flow rate of the jets on the pressure distributions over the wing, for two chord positions. One of them (Figure 11) was very close to the axis of the jet and the second one was farther away (Figure 12). In the latter case, theinfluence of the delay rate of the jet is completely negligible.

3.2 Nacelle-wing interaction on the pressure distributions

Figure 13 shows the effect of the presence of the wing on the pressure distributions over the nacelle fairing FSC for two Mach numbers. The influence is substantial, especially at Mo = .794.

Figures 14 and 15 show the influence of the presence of the nacelle FSC on the pressure distributions over the wing for two chord values. The effect is pronounced for the central section (Figure 14) which is not surprising. It is also the same for the more distant section (Figure 15). The effect is translated especially for this chord distance by a movement upstream of the shock on the topside of the wing.

3.3 Influence of the relative wing-nacelle position

3.3.1 Influence of the horizontal position

Figure 16 shows the variation of C_x of the wing and the thrust coefficient of the nacelle caused by a horizontal displacement of the wing and nacelle.

We find that the drag of the wing and the thrust of the nacelle are increasing functions of the relative distance. The global interaction balance represented in Figure 16 is always favorable and shows that the best position is the 21' which is where the wing and the nacelle are closest to one another.

3.3.2 Influence of the vertical position

Figure 17 shows that when the wing is displaced vertically away from the nacelle, the drag of the wing and the thrust of the nacelle decrease slightly. The global interaction balance, which is always favorable, indicates that the most distant position is

the best but the change from the other positions is only small.

The results of the two paragraphs above confirm those in [16].

3.3.3 Study of pressure distributions over the nacelle

Figure 18 shows the variation of the pressures over the nacelle for various relative positions studied for cruise flow rate. The pressure level over the secondary fairing increases when one moves the wing away from the nacelle horizontally or vertically to position 21', except for the last pressure tap.

3.4 Influence of the nacelle type

The two nacelle types FSC and FCC were compared with the wing in a similar position, that is for two distances of the central profile leading edge of the wing from the reference plane of models of identical nacelles. /20-5

Compared to the FSC nacelle in position 10, nacelle FCC brings about a strong reduction in the drag. The presence of the wir ; the same effect on the thrust of the two nacelles which gives a more favorable global thrust-drag balance for the FCC nacelle (see Figure 19).

3.5 Influence of the presence of the pylon

Two confi rations which only differed by the presence or the absence of the pylon were compared. The nacelle is the same (FSC) as is the relative wing-nacelle position (21'). The incidence, the Mach number upstream (0.794) and the delay flow rate of the jets are also the same.

Figure 20 shows the difference between the pressure distribution over the wing for $\eta = 0.456$. We find that locally on the bottom

side, the presence of the pylon provokes a substantial acceleration of the flow.

When one moves away in the chord direction, at $\eta = 0$ (Figure 21), the influence of the presence of the pylon on the pressure distribution is negligible.

4. DISCUSSION OF RESULTS

The results presented here will consider again the local and global C_x values obtained by integration of the pressures over the wing. They have to be confirmed by the determination of the C_x obtained by sounding of the wakes of the wing. The tests were performed during a second test campaign and the results have not yet been analyzed.

Also, the study of the relative wing-nacelle position was performed without a pylon. The importance of the pylon, emphasized in Section 3.5, will require the study of the presence of the pylon. Unfortunately, the type of installation used here is not very practical for such a study (one has to build a pylon shape for each position of the nacelle).

As far as the measurement of the thrust of the rear body is concerned, the configuration was calibrated using a calibration nozzle of the ASME type which is shown in Figure 22. The tests were performed for two external Mach numbers and expansion flow rates which varied and these were compared with results obtained with a similar nozzle tested on the dynalpy BD2 test stand of the ONERA at Modane. Also, a formula proposed by ASME was used. Figure 23 summarizes the comparisons and shows that the agreement is good, both for the isentropic thrust coefficient η_μ and the flow rate coefficient C_D, which validates the relative results of the thrust.

5. CONCLUSION

A nacelle-wing interaction test configuration has been developed for the S3Ch wind tunnel of the ONERA for subsonic configurations to be used in the future. That is, we are testing the supercritical wing and double flux engine nacelles with a high dilution rate. The characteristics of the wing are determined by measuring wall pressure distributions on eight sections, by using wake soundings downstream of the sections. The nacelles are placed downstream of an upstream wing which carries compressed air flow. The thrust of the rear body and the flow rate coefficient of the nozzle are measured. The study of the effect of various parameters can then be carried out:

- expansion ratio of the jet engine;
- upstream Mach number;
- relative wing-nacelle position;
- nacelle type;
- presence of the pylon.

The results presented illustrate the multiple possibilities of this installation which can be used in the future:

- on the one hand, to facilitate our understanding of interaction phenomena;
- on the other hand, to validate the corresponding theoretical prediction methods.

NOTATION

/20-6

B	1/2 chord of the wing
C	chord of the wing
C_D	nozzle flow rate coefficient
C_x	drag coefficient
C_{xp}	pressure drag coefficient of the wing carrying the pressure taps
C_z	lift coefficient of the part of the wing carrying the pressure taps
D	diameter of the nacelle in the secondary ejection plane
C_{As}	thrust coefficient of the nacelle
K_p	pressure coefficient $K_p = \frac{p - p_o}{Q_o}$
K_x	local drag coefficient of one wing section
K_z	local lift coefficient of one wing section
M_o	upstream Mach number
p	local static pressure
p_o	reference static pressure
p_i	local stagnation pressure
p_{io}	reference generating pressure
p_{is}	stagnation pressure of secondary jet
Q_o	reference dynamic pressure $Q_o = 0,7\, p_o M_o^2$
R_N	Reynolds number measured in the calibration nozzle throat
S	wing reference area
x	abscissa measured over one meridian of the nacelle (origin for the nacelle reference plane)
X	abscissa of the secondary ejection plane (B.A. origin of the central wing chord)
Y	chord distance (origin: section no. 8 of the wing)
Z	vertical distance (origin: test section axis)
α	incidence angle of wing
$\eta = \frac{Y}{B}$	reduced chord
η_μ	isentropic thrust coefficient

ABBREVIATIONS

FCC	short confluent flux nacelle
FSC	short separate flux nacelle
FCL	long confluent flux nacelle

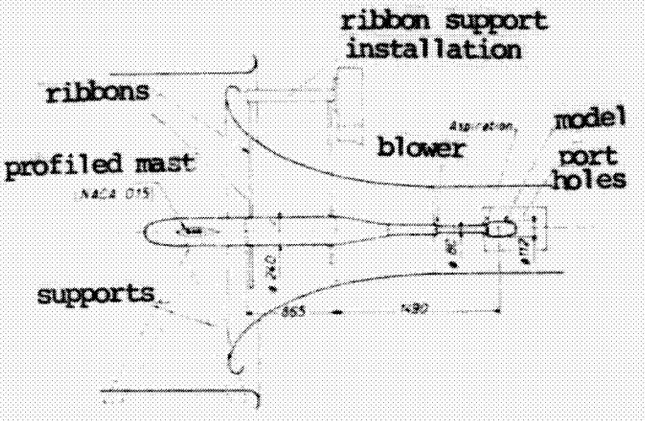

FIGURE 1. Diagram of the D4 installation

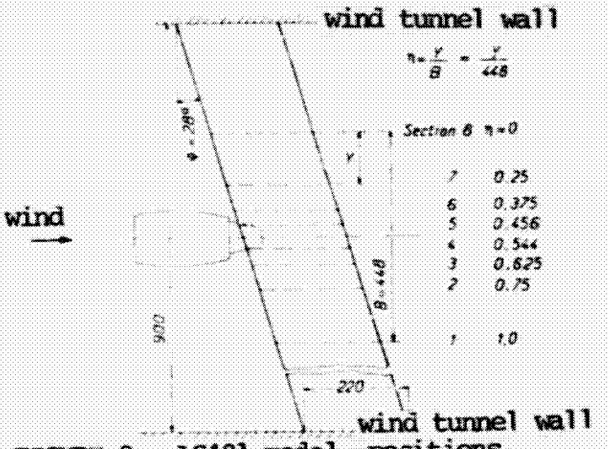

FIGURE 2. AS401 model—positions of the pressure measurement section

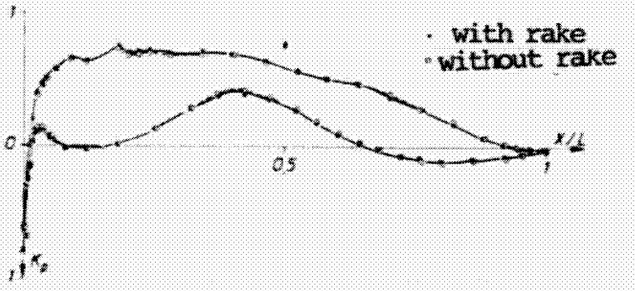

FIGURE 3. Influence of the presence of the wake sounding rake on the pressure distribution over the wing. $M_\infty = 0.794$; $\alpha = 1°$; $\eta = 0.544$. Position 25 without pylon. FSC cruise nacelle.

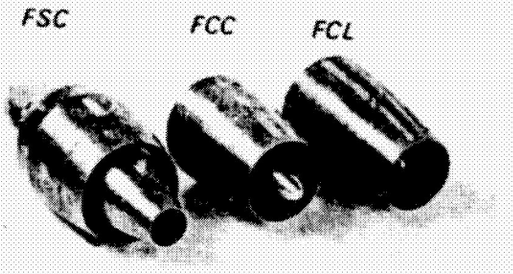

FIGURE 4. After body CFM 56 models

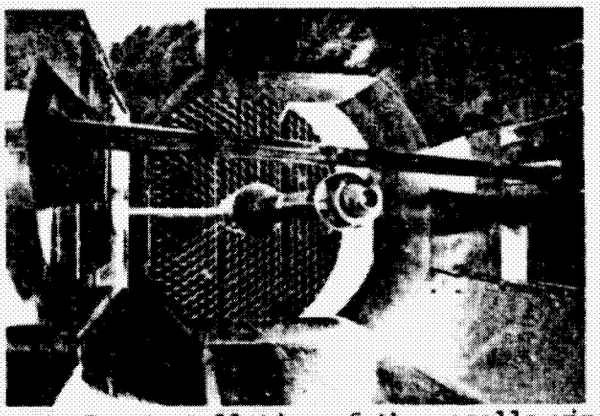

FIGURE 5. Installation of the nacelle-wing interaction test assembly in the S3Ch ONERA wind tunnel

	X	X/C	Z	Z/D
10	26,5	0,12	21,5	0,18
11	26,5	0,12	29,85	0,25
13	26,5	0,12	44,28	0,37
14'	50,73	0,23	21,5	0,18
21'	0,21	0,001	21,5	0,18
25	24,78	0,11	21,5	0,18

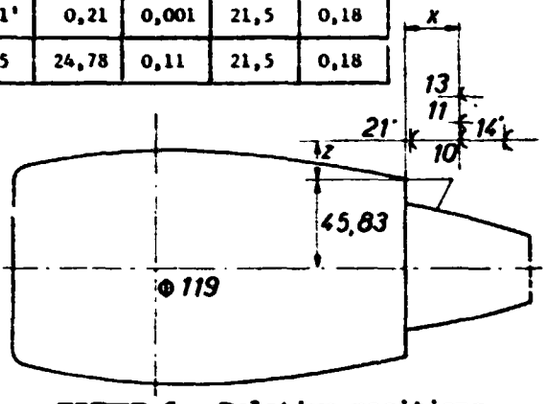

FIGURE 6. Relative positions studied. FSC nacelle.

	X	X/C	Z	Z/D
15	- 50,94	- 0,23	29,5	0,39
16'	- 65,21	- 0,30	29,5	0,39
17	- 50,94	- 0,23	39,75	0,52
18'	- 21,15	- 0,10	29,5	0,39

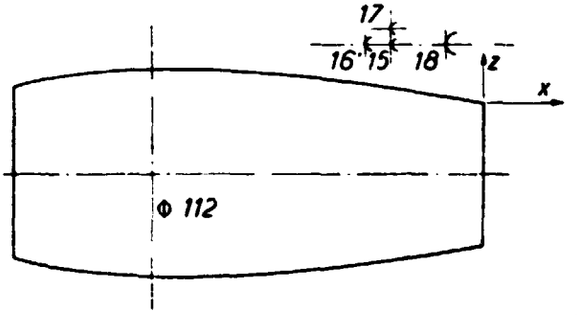

FIGURE 7. Relative positions studied. FCC nacelle.

	X	X/C	Z	Z/D
23	- 22,35	- 0,1	36,93	0,53
24	- 50,98	- 0,23	32,33	0,46

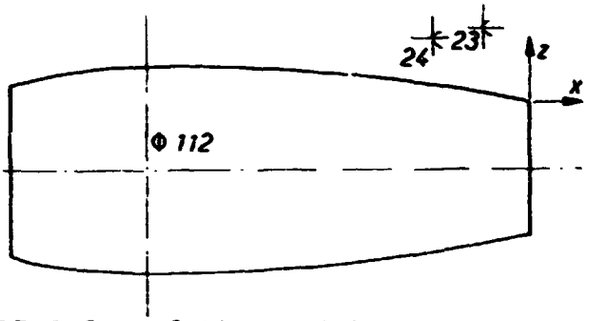

FIGURE 8. Relative positions studied.
Nacelle FCL.

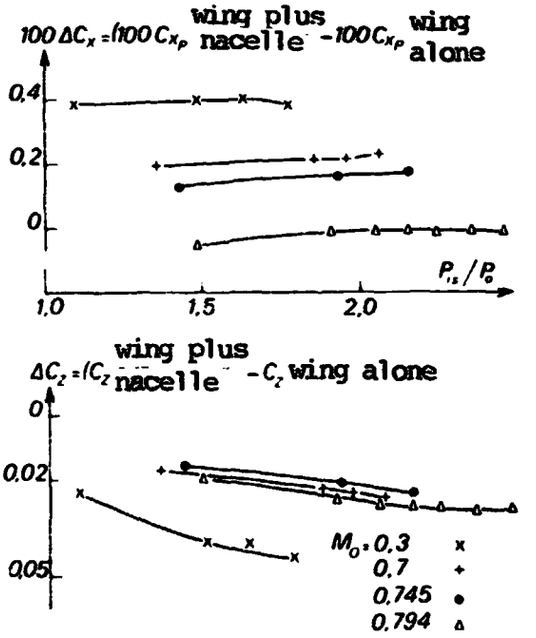

FIGURE 9. Influence of the jet delav rate.
Position 10. FSC nacelle $\alpha = 1^{\circ}$

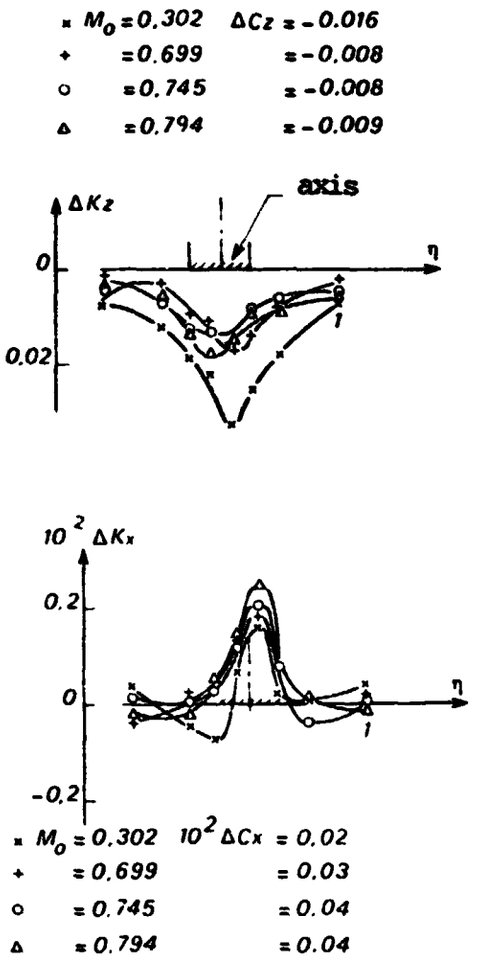

b

FIGURE 10. Influence of the Mach number on the C_x and C_z distributions of the wing as a function of chord distance. FSC nacelle. Position 10. $\alpha = 1°$

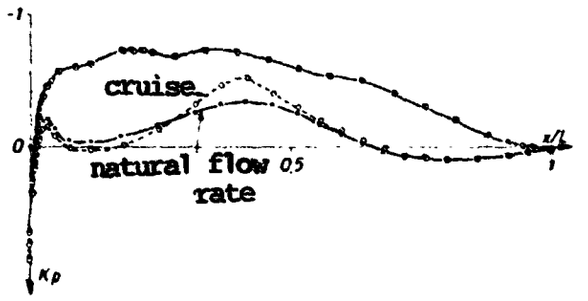

Figure 11. Influence of the expansion ratio of the jet on the pressure distributions over the wing. $M_o = 0.794$; $\alpha = 1°$; $\eta = 0.544$

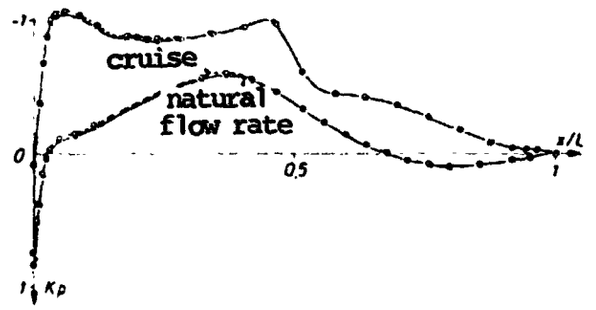

FIGURE 12. Influence of the expansion ratio of the jet on the pressure distributions over the wing. $M_o = 0.794$; $\alpha = 1°$; $\eta = 0$. Nacelle FSC in position 10.

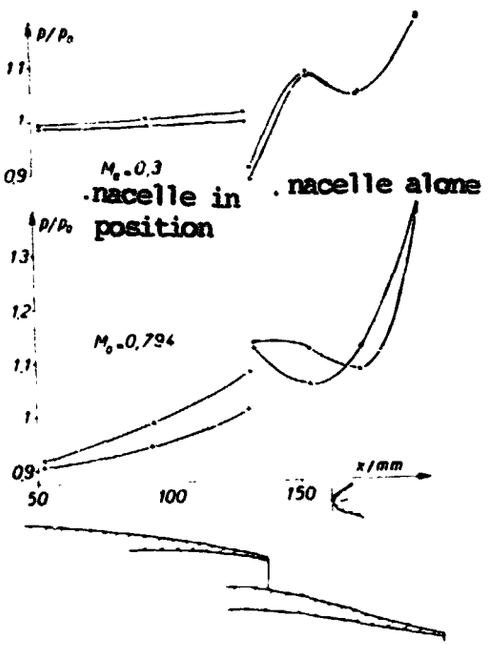

FIGURE 13. Influence of the presence of the wing on the pressure distributions over the FSC nacelle in cruise

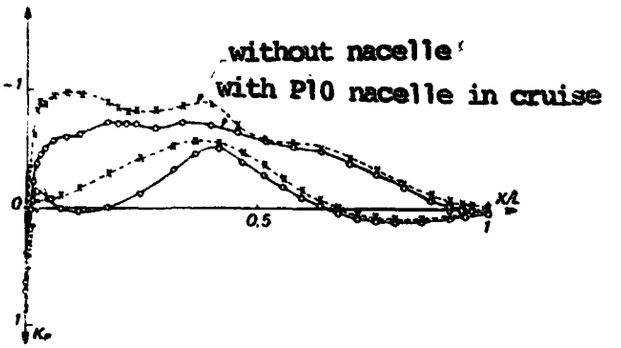

Figure 14. Influence of the presence of the nacelle on the pressure distribution over the wing. $M_o = 0.794$; $\alpha = 1°$; $\eta = 0.544$

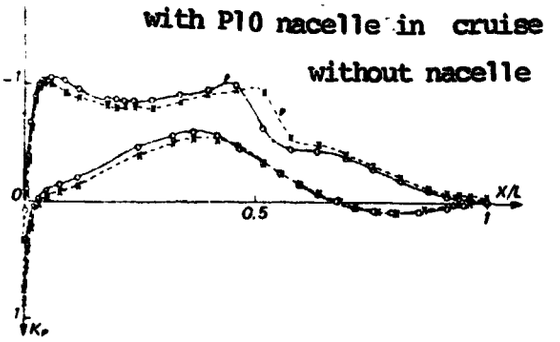

Figure 15. Influence of the presence of the nacelle on the distribution of pressure over the wing. $M_o = 0.794$; $\alpha = 1°$; $\eta = 0$

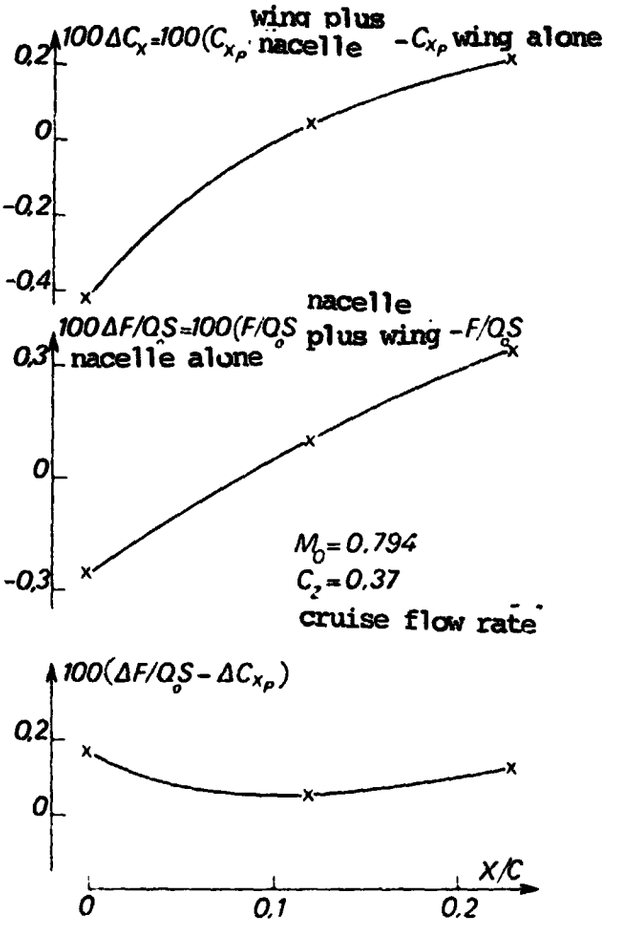

FIGURE 16. Influence of the relative horizontal position.

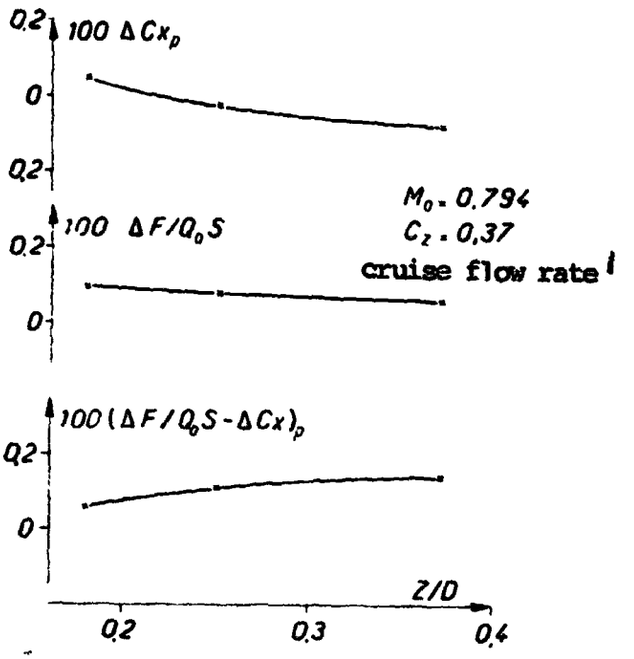

FIGURE 17. Influence of the relative vertical position.

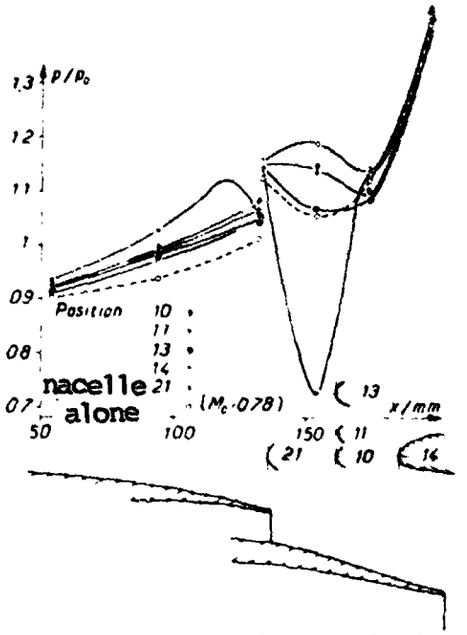

FIGURE 18. Influence of the relative wing/nacelle position on the pressure distributions over the nacelle FSC
M_0 = 0.794; α = 1°, cruise

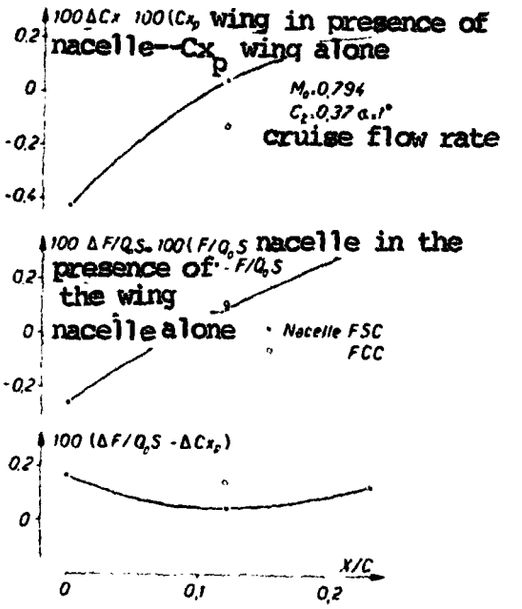

FIGURE 19. Influence of the nacelle type

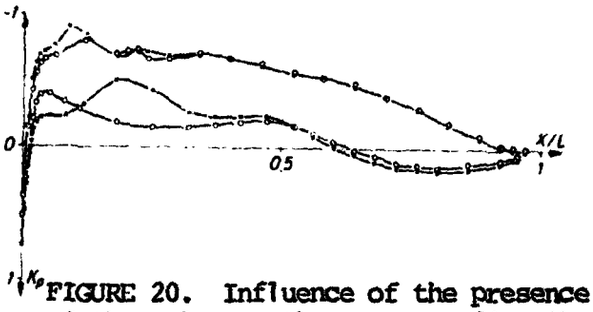

FIGURE 20. Influence of the presence of the pylon on the pressure distribution over the wing $M_0 = 0.794$; $\alpha = 1°$; $\eta = 0.456$. Nacelle position 21'. Cruise flow rate.

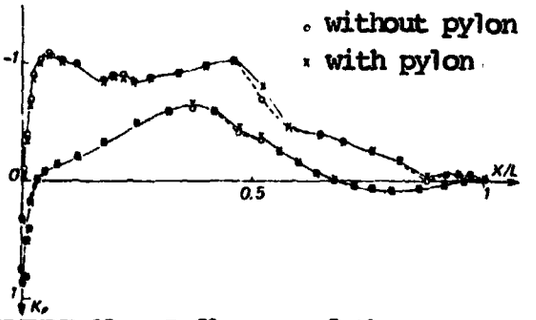

FIGURE 21. Influence of the presence of the pylon on the pressure distribution over the wing. $M_\infty = 0.794$; $\alpha = 1°$ $\eta = 0$. Nacelle FSC position 21'. Cruise flow rate

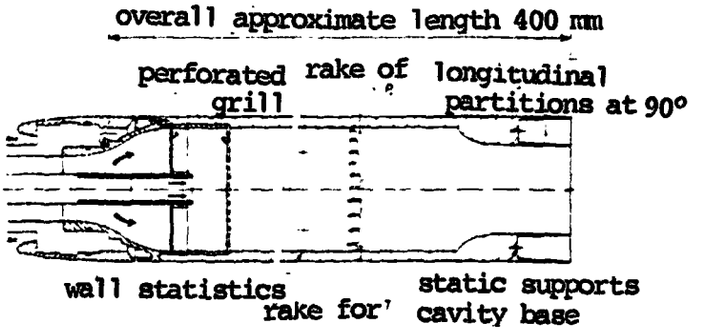

FIGURE 22. S3 Chalais reference nozzle installation

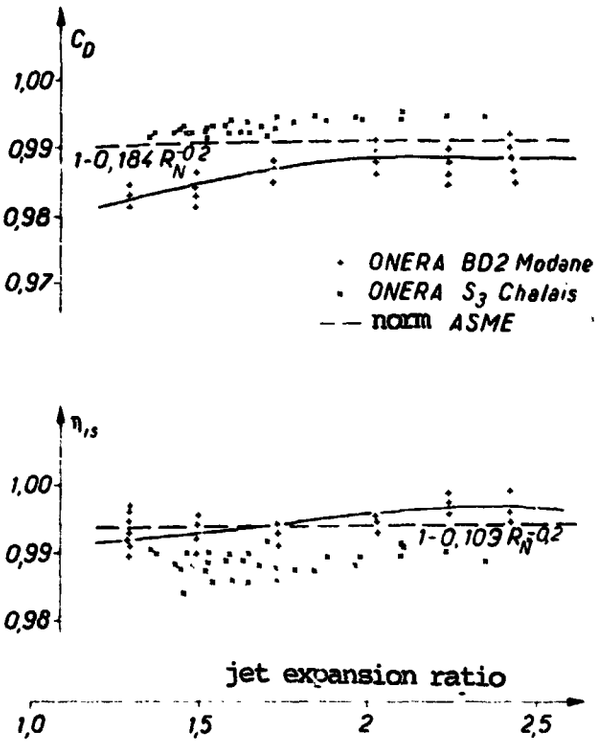

FIGURE 23. Comparison of tests ot a reference ASME nozzle

REFERENCES

1. Kho, Y. G. Wind-tunnel measurements on the interference between a jet and a wing, located outside the jet. Part I. NLR TR 77009 U.

2. Zandbergen. Experimental investigation of the aerodynamic characteristics of a wing in propulsive jets. NLR TR 77081.

3. Wittmann, M. and Fischeder, W. Institut fuer Luft-und Raumfahrt, TH Aachen. Investigation of the interaction between engine nacelle and wing. DLR FB 74-32, 1974.

4. Swan-Sigalla. The problem of installing a modern high bypass engine on a twinjet transport aircraft. AGARD CP-124.

5. Kuhney. Airframe/propulsion system integration analysis using the propulsion simulator technique. AGARD CP-71-71.

6. Saiz. Interaction des jets des réacteurs GE CF6 50 sur la cellule de l'Airbus en croisière Simulation en soufflerie (Bordeaux) (Interaction of GE CF6 50 engine jets with the AIRBUS airframe under cruise conditions. Wind tunnel simulation (Bordeaux) AAAF 1974.

7. Patterson, J. A wind tunnel investigation of jet wake effect of a high bypass engine on wing nacelle interference drag of a subsonic transport. NASA TND 4693.

8. Munniksma - Jaarsma. Jet interference of a podded engine installation at cruise conditions. AGARD CP 150.

9. Krenz, G. Airframe engine interaction for engine configurations mounted above the wing. Part I: interference between wing and intake/jet. AGARD CP 150.

10. Ewald, B. Part II: engine jet simulation problems in wind-tunnel tests. AGARD CP 150.

11. Raney, D. J., Kurn, A. G. Wind tunnel investigation of jet interference for underwing installation of high bypass ratio engine RAE TR 68049 1968.

12. Pauley, G. Interim note on tests with a wing mounted fan nacelle with the fan jet simulated by cold air blowing and alternatively by a gas generator shroud. ARCCP 1111.

13. Paterson Flechner. Jet wake of a high bypass engine on wing nacelle interference drag of a subsonic transport airplane NASA TN D 6067 (1970.

14. Pindzola, M., Lo, C. F. Boundary interference at subsonic speeds in wind tunnels with ventilated walls. AEDC TR 69.47 - May 1969.

15. El Ramly, Z., Rainbird, V. J. Effect of simulated jet engines on the flowfield behind a swept back wing. Journal of Aircraft Vol. 14 no. 4, April 1977, p. 343-349.

16. Aldridge, S. E., Nye, J. L. Experimental results of high bypass ratio turbofan and wing aerodynamic interference AGARD CP 71.